Newberry Volcano EGS Demonstration Stimulation Modeling

Trenton T. Cladouhos, Matthew Clyne, Maisie Nichols,
Susan Petty, William L. Osborn, and Laura Nofziger
AltaRock Energy, Inc.

Keywords: stimulation model, EGS, Newberry, AltaStim, hydroshear, fracture model

Abstract

As a part of Phase I of the Newberry Volcano EGS Demonstration project, several data sets were collected to characterize the rock volume around the well. Fracture, fault, stress, and seismicity data has been collected by borehole televiewer, LiDAR elevation maps, and microseismic monitoring. Well logs and cuttings from the target well (NWG 55-29) and core from a nearby core hole (USGS N-2) have been analyzed to develop geothermal, geochemical, mineralogical and strength models of the rock matrix, altered zones, and fracture fillings (see Osborn et al., this volume).

These characterization data sets provide inputs to models used to plan and predict EGS reservoir creation and productivity. One model used is AltaStim, a stochastic fracture and flow software model developed by AltaRock. The software's purpose is to model and visualize EGS stimulation scenarios and provide guidance for final planning. The process of creating an AltaStim model requires synthesis of geologic observations at the well, the modeled stress conditions, and the stimulation plan. Any geomechanical model of an EGS stimulation will require many assumptions and unknowns; thus, the model developed here should not be considered a definitive prediction, but a plausible outcome given reasonable assumptions. AltaStim is a tool for understanding the effect of known constraints, assumptions, and conceptual models on plausible outcomes.

Theoretical Overview

AltaStim is a software implementation of the equations developed in Willis-Richards et al. (1996), and Jing et al. (2000). At the heart of the model is 1) a rule for determining when hydroshearing occurs, 2) an equation to adjust the aperture of a hydrosheared fracture, and 3) a summation to calculate the directional fracture permeability that controls the overall growth of the stimulation volume.

Hydroshearing on a pre-existing fault plane occurs when the fluid pressure (**P**) reduces the effective normal stress ($\boldsymbol{\sigma_{eff}}$) such that the shear stress on the plane ($\boldsymbol{\tau}$) is exceeded,

$$\boldsymbol{\sigma_{eff}} = \boldsymbol{\sigma_n} - \mathbf{P} \qquad \text{Equation 1}$$

$$\boldsymbol{\tau} < \boldsymbol{\sigma_{eff}}\,\boldsymbol{\mu} \qquad \text{Equation 2}$$

where $\boldsymbol{\sigma_n}$ is the stress normal to the fault plane and $\boldsymbol{\mu}$ is the coefficient of static friction on the fault plane.

The aperture of a hydrosheared fracture is determined from Equation 14 of Willis-Richards et al. (1996),

$$\mathbf{a} = \frac{\mathbf{a_0 + U \tan \varphi_{dil}}}{\mathbf{1 + 9\sigma_{eff}/\sigma_{nref}}} \qquad \text{Equation 3}$$

where **U** is shear displacement, $\mathbf{a_0}$ is initial aperture, $\boldsymbol{\varphi}_{\mathbf{dil}}$ is shear dilation angle, and $\boldsymbol{\sigma}_{\mathbf{nref}}$ is the closure stress.

The increase in directional permeability ($\mathbf{\Delta K_i}$) due to the i^{th} hydrosheared fracture is proportional to the aperture (**a**) and the angle ($\boldsymbol{\theta}$) between the fracture and the direction in which permeability is being calculated.

$$\mathbf{\Delta K_i \sim a_i^3 \cos^2 \theta} \qquad \text{Equation 4}$$

To calculate the relative bulk fracture permeability of a part of the model, the equation above is summed over all fractures in that part of the model.

The reader is referred to the technical papers for more details of these governing equations for the AltaStim model. The model run proceeds in the following steps:

1. The user inputs a fracture model, rock mechanics parameters, native-state stress conditions (three principle magnitudes and directions), and the initial hydrostatic fluid pressure.
2. The software starts with a random center and determines fracture orientation, aperture and length parameters from either a statistical model or a list of actual fractures observed in the borehole (bootstrapping). The shear stress and normal stress are calculated for each fracture. Fracture generation continues until the goal of fracture porosity or fractures intersected in a simulated well is reached.
3. The user inputs the wellhead pressure (WHP) to be applied to the modeled well.
4. EGS reservoir creation modeling begins by testing each fracture near the well bore to determine whether it will hydroshear by comparing the coefficient of sliding friction, normal stress, shear stress, and fluid pressure (Equations 1 and 2). If a fracture does hydroshear, then a seismic event is recorded and the fracture aperture increases (Equation 3).
5. The EGS reservoir grows away from the well based on the calculated fracture permeability in sectors about the well (Equation 4).
6. The model continues testing fractures for hydroshearing, and increasing the dimensions of the EGS reservoir until the long dimension of the reservoir reaches 550 m (the reservoir length goal plus 10%) or after 700 AltaStim cycles (a stalled stimulation).
7. AltaStim outputs include total fracture volume, a 3D image of the seismic events and vectors, and the status of each of the tested fractures (resolved shear stress, normal stress, fluid pressure, aperture, number of seismic events, etc.).

Newberry EGS Model Dimensions and Zones

For the Newberry EGS AltaStim model, the horizontal dimensions are 700 m east-to-west and 1100 m north-to-south. A rectangular shape was used because, as expected, the reservoirs tended to grow north-south due to the fracture and stress orientations.

The thickness of the models varied depending on the zone or depth range being modeled. The open hole was divided into five zones based on borehole televiewer (BHTV) fracture intensity, lithology, mud losses while drilling, and water losses during the injection tests. The characteristics of these zones are summarized below in Table 1. Each of these zones requires different inputs for fracture orientations and intensity.

Table 1: Summary of geologic zones identified in NWG 55-29.

Zone	**Depth to Zone Center (m) /zone thickness**	**Fracture Count in Zone / Intensity in well (#/m)**	**Lithology**	**Mud Losses during drilling**
A	1978 / 86	5 / 0.06	Primary: Welded Lithic Tuff Secondary: Other Tuff	None
B	2201 / 360	173 / 0.4	Primary: Tuffs Secondary: Basalt, Dacite, and Andesite	< 50 bbl
C	2481 / 200	157 / 0.8	Primary: Basalt and Basaltic Andesite Secondary: Two Felsic Dikes,	< 20 bbl
D	2712 / 262	16 / 0.06	Primary: Microcrystalline Granodiorite (5 dikes, 570 ft total) Secondary: Basalt, one large (50) felsic dike	None
E[1]	2922 / 200		Primary: Basalt Secondary: Three felsic Dikes	> 100 bbl

[1]Zone E was not visualized by the BHTV survey. The motor quit working due to the high temperatures at this depth.

Orientations, Apertures, Intensity, and Size

One approach for generating fractures is to determine statistical models for fracture orientation, apertures, and sizes based on the analysis of the data, and then to use those statistics to generate fractures. A simpler approach, commonly called *bootstrapping*, is to draw attributes from a list of the actual fractures identified in the BHTV image. For the Newberry model, the 351 fractures identified in the BHTV images are divided into separate lists by zones and used to populate the

fracture orientations and apertures in the model for each zone. Fractures are added to the modeled zone until fracture intersections in a modeled well reaches the same count as the real well in that zone.

The initial fracture apertures were assigned to account for the very low fracture permeability currently observed. After hydroshearing, the maximum fracture aperture in the models was about 5 mm with an average aperture of about 1.5 mm. Fracture radius (size) is a very difficult parameter to determine from well data, since all that is known for certain is that the fracture is bigger than the well bore diameter. For the purpose of the AltaStim models, a uniform distribution of radii between 33 and 120 m was used. The lower limit keeps the total number of fractures in the model to a computationally acceptable number and the upper limit prevents any fractures from cutting fully across the model space.

Coefficients of Sliding Friction

The fluid pressure at which hydroshearing initiates will depend on the coefficient of sliding friction (μ) (Equation 2), which is also sometimes expressed as the angle of friction θ_f, where $\mu = \tan \theta_f$. The constraints on friction are mostly related to the rock types described in the mud logs. Zones A and B are dominated by silica-rich extrusives (tuffs, rhyolites, and dacites). Mechanical testing of a similar suite of rocks from Yucca Mountain indicate that these rocks are likely to have a relatively high coefficient of sliding friction (μ=0.85, θ_f=40°) (Morrow and Byerlee, 1984). Therefore, a coefficient of sliding friction in these two zones of 0.85 was used.

Zone C and E are dominated by basalts with more plagioclase and less quartz than the overlying extrusive rocks. There is evidence for localized contact metamorphism and alteration in these zones, which may have created weaker layered minerals like chlorite along fractures and contacts. Therefore, a moderate sliding friction of μ=0.70 (θ_f=35°) is set in Zones C and E (Lockner and Beeler, 2002).

Zone D has the most evidence for localized contact metamorphism along the margins of the granodiorite dikes. Therefore, a relatively low sliding friction of μ=0.64 (θ_f=32.5°) is set in Zone D (Lockner and Beeler, 2002).

The coefficients of sliding friction chosen above are consistent with the hypothesis that 1) Zones A and B are far from failure and were unaffected by the increase to 1153 psi (7.9 MPa) during injection testing (Osborn et al., this volume), 2) Zones C and E are closer to failure as indicated by drilling mud losses and fluid loss during injection, and 3) Zone D was in incipient failure at a WHP of 1153 psi as indicated by the change in temperature logs between two injection tests conducted at 750 psi (5.2 MPa) and 1153 psi WHP.

Stress

Stress orientation in boreholes can be determined from the fracturing or breakouts caused by compressional failure of the borehole walls. In NWG 55-29, the breakouts show a consistent azimuth indicating that the minimum horizontal stress, S_{hmin} is oriented at 092 ±16.6° relative to

true north. This azimuth of S_{hmin}, in combination with the attitude of the majority of natural fractures revealed in the image log, is consistent with normal faulting. The consistency of breakout azimuth, without localized rotations, taken in combination with the extremely low rate of seismicity in the region and the weak expression of natural fractures in the image log, suggests that there is little recent or active slip on fractures in the vicinity of the well (Davatzes and Hickman, this volume).

Determining the magnitudes of the three principle stresses is more difficult. In a normal faulting regime, the maximum principle stress is vertical (S_v) with a magnitude related to the weight of the lithostatic overburden. The minimum horizontal stress (S_{hmin}) at a given depth is best determined from a mini-frac, a well test in which S_{hmin} is determined from the fluid pressure at which tensile fracturing occurs. An accurate mini-frac requires a short (~50 ft, 15 m) section of relatively unfractured well bore to be isolated. Isolation allows for sufficient pressure build-up to cause tensile fracturing, provides a narrow depth range over which to calculate S_{hmin}, and ensures that the measured pressure response is due to a tensile failure and not hydroshearing. Because NWG 55-29 has over 3000 feet (>1000 m) of open hole and isolating a short section would require a drilling rig, it is not feasible to conduct a mini-frac to determine S_{hmin}. Instead, S_{hmin} must be constrained based on reasonable geomechanical assumptions. The magnitude of the maximum horizontal (S_{Hmax}) is also difficult to determine, but is constrained to lie between S_v and S_{hmin}. The wide borehole breakout widths over most depths in NWG 55-29 indicate that the horizontal stress difference ($S_{Hmax} - S_{hmin}$) is relatively large (Davatzes and Hickman, this volume).

Two stress cases were used to develop input parameters (Table 2) for the AltaStim models, with each case representing a different hypothesis of the deformation that occurred during the injection test that reached 1153 psi WHP. In the first case, in which a gradient of 0.66 psi/ft (14.9 MPa/km) for S_{hmin} is used, the model predicts that a few ideally oriented fractures would have hydrosheared at 1153 psi WHP, to account for changes observed in temperature logs run during the injection. In the second case, in which a gradient of 0.7 psi/ft (15.8 MPa/km) for S_{hmin} is used, no hydroshearing is predicted by the model at 1153 psi WHP.

Table 2: Stress inputs to AltaStim models.

Component	**Gradient (MPa/km)**	**Gradient (psi/ft)**	**Direction**	**Principle Stress**
S_V gradient	24.1	1.07	vertical	maximum
S_{Hmax} gradient	23.5	1.04	2° (N-S)	intermediate
S_{hmin} gradient	14-9 - 15.8	0.66 -0.70	92° (E-W)	minimum
P_h gradient	8.8	0.39	-	-

Deterministic Features in Zone D

Zone D presents special complications for modeling. The BHTV images of this zone are of a lower quality than shallower zones because the images were collected on the way down at a higher rate of descent in order to log as deeply as possible before the tool reached its maximum temperature and stopped working. The higher logging speeds greatly reduce vertical tool resolution. The top 200 feet of Zone D is within microcrystalline granodiorite, a unique rock type in the BHTV image log. In the BHTV images, the granodiorite contains no borehole breakouts and a low fracture intensity, indicating that the granodiorite is relatively strong.

In contrast to the observations of greater strength and sparse fracturing in the top 200 feet (60 m) of Zone D, this zone appears to be the depth in which most of the water loss during the injection test occurred. One explanation for the apparent contradiction is that the intrusive contacts between the granodiorite and the country rock (basalts) are commonly altered or chloritized, according to the mud log.

Thus, an AltaStim model of Zone D was built to account for the potential role that the intrusive contacts may play during EGS stimulation. Unlike the fractures modeled in the other zones, which have stochastic locations, the depths of these contacts are known from the mud logs. The contacts are likely to extend far from the well bore; therefore, AltaStim's deterministic features model was used to represent the intrusive contacts. Two orientations were measured on the BHTV image at the top of the first granodiorite dike – the only large dike contact that was reached by the BHTV. These orientations are alternated for all the dikes in the model. The dikes are considered to be major features that will extend outside of the Zone D model volume; therefore, they are given a radius of 200 m.

Stochastic Realizations

AltaStim generates random locations for fractures. Each run of the AltaStim model with the same parameters but different random seeds, called realizations, has different initial conditions that will control how details of the stimulation process proceeds. Even separate runs of the Zone D model, which contains five deterministic fractures, produce different results due to the background fractures also in the model.

In well-constrained, mature models, it is preferable to generate a sufficient number of realizations (10-100) to develop statistics, standard deviations, and confidence intervals. The modeling effort reported here focuses on developing the initial model inputs; therefore, the number of realizations was kept to a minimum. The results below are based on three realizations for each model scenario. Even with the limited number of realizations, a wide range of results were produced.

Model Outputs

An AltaStim model run produces synthetic outputs for each fracture (shear slip, final aperture, and resolved stress components) and model-wide outputs (total fractures tested, hydrosheared,

and distance of stimulation from well bore). The following parameters are tracked and reported below:

Total fracture volume – The fluid volume for an individual fracture is calculated by multiplying the sheared aperture by the fracture area ($a\pi r^2$). The total fracture volume is calculated by summing across all the fractures which have been stimulated. It is assumed that in impermeable rocks, all injected fluid volume goes into filling the hydrosheared fractures. This *parallel plate assumption* for fractures is a simplification between two possible end-members. First, the assumption *underestimates* the volume injected because some fluid will leak off into secondary features, non-sheared fractures, and even the rock matrix. Second, the assumption *overestimates* the volume injected because real sheared fractures are not circular nor do they have the same aperture everywhere on the fracture surface. Theoretically, the maximum aperture will be at the wellbore face and decrease to zero at the fracture tips. Observationally, natural fracture surfaces tend to be rough, with variable apertures on a short length scale. The natural roughness of fracture surface means that fluid will likely flow along channels on the fracture surface, rather than between parallel plates.

Reservoir shape –The reservoir shape is tracked by plotting the 'seismicity' generated each time a fracture is hydrosheared. Each seismic event has a location that can be displayed in a 3D plotting program. Reservoir shape is also tracked by the set of vectors whose growth in each cycle is determined from its relative fracture permeability. When the longest vector reaches 550 m, long dimension from the center of the model region, the model run is over.

Mohr Circle – Stress is not easy to visualize because, in the 3D case, it is a 3x3 tensor that can only be simplified to three principal stress magnitudes and directions. The Mohr Circle for 2D stress is one method used to visualize a state of stress. It is used here to show the relationship between the effective (fluid weakened) stress state and the frictional failure envelope. Hydroshearing for a fracture of a given orientation is indicated when the shear stress and effective normal stress coordinates for that fracture plot to the left of the friction sliding failure envelope. As fluid pressure increases and lowers the effective normal stress on all fractures, more fractures orientations will cross the failure envelope and become favorably oriented for hydroshear.

Wellhead Pressure - The wellhead pressure (WHP) was the primary input that was varied in the model runs. The modeled stimulations began at the injection test pressure of 1153 psi WHP and continued to a pressure sufficient to reach EGS reservoir length goal (1950-2350 psi depending on the stress case). To remain in the hydroshearing regime, WHP in the models was kept low enough to prevent exceeding the minimum principle stress in almost all model runs.

Results

The overall results of the modeling can be summarized on a graph of WHP versus the total volume of the fractured reservoir (Figure 1). The average aperture of the hydrosheared fractures

in all the models is between 1 and 1.5 mm; therefore, the differences in fracture volumes are simply related to the total number of hydrosheared fractures in each model run. A volume goal of 5 million gallons was added to the length goal of 550 m to ensure that a reservoir of sufficient size with a cloud-like shape was created. The model was able to reach the length goal by creating linear stimulated features, so the volume goal was added to control the shape of the stimulated area.

Overall, the modeling indicates that Zones C, D, and E have sufficient fracturing to reach the volume goal of over 5 million gallons. In the 0.66 psi/ft S_{hmin} stress case, significant hydroshearing begins at 1350 psi WHP and over 1950 psi WHP is required to consistently reach the volume goal. In the 0.70 psi/ft S_{hmin} stress case, hydroshearing begins at a WHP of 1350 psi and over 2200 psi was needed to reach the volume goal. Zone D is consistently the zone which takes the most fluid at the lowest pressure; a result of a model populated with deterministic dikes and an assumed lower coefficient of sliding friction. The deterministic features were added to Zone D in order to satisfy the observation that the interval may have been in incipient failure during the injection tests at 1153 psi.

The results for each zone and their implications are discussed in more detail below. In particular, graphical results for Zone C are more completely covered as this zone's high fracture intensity and variety of fracture orientations make the model results the clearest.

Zone A

The low fracture intensity in the Zone A models limited the average number of hydrosheared fractures to less than 10 out of an average of 1266 fractures in the model space, even at the highest WHP in both stress cases. The average volume injected in this zone was less than 35,000 gallons in every case.

Zone B

The moderate fracture intensity in the Zone B model allowed for significantly more stimulated volume in Zone B than Zone A. However, the volume goal was not met for this zone at any pressure. One reason for this is that the Zone B models were often asymmetric; that is, the EGS reservoir would grow in only one direction from the well. Like the model, the actual stimulation may also stall for lack of connectivity due to the low fracture intensity in Zone B.

Zone C

The wide range of fracture orientations and high fracture intensity make Zone C the most instructive for understanding the impact of increased fluid pressure in an AltaStim model and the hydroshearing process. At 1153 psi, a few fractures are in contact with the failure envelope but too few to propagate away from the well bore. At a WHP of 1350 psi, less than 20% of the tested fractures were found to hydroshear, resulting in a narrow simulated EGS reservoir that reached the length goal of 550 m, but not the volume goal of over 5 million gallons (>19,000 m^3)(Figure 1 – top). At a WHP of 1950 psi for the 0.66 psi/ft S_{hmin} stress case, approximately half of the

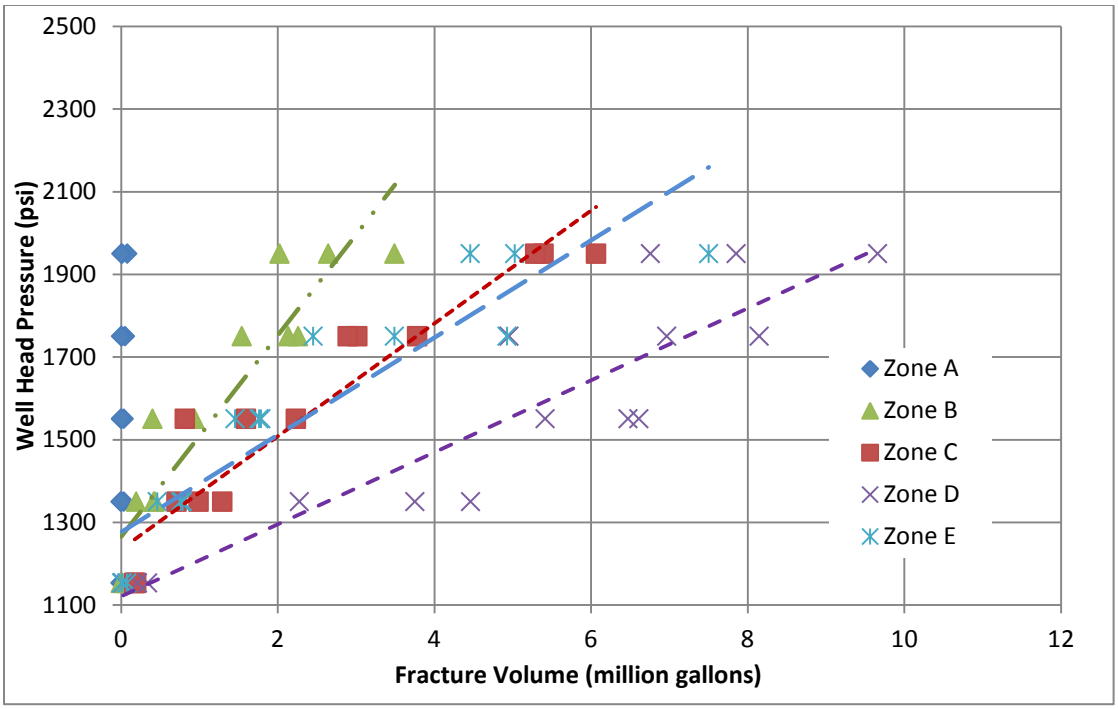

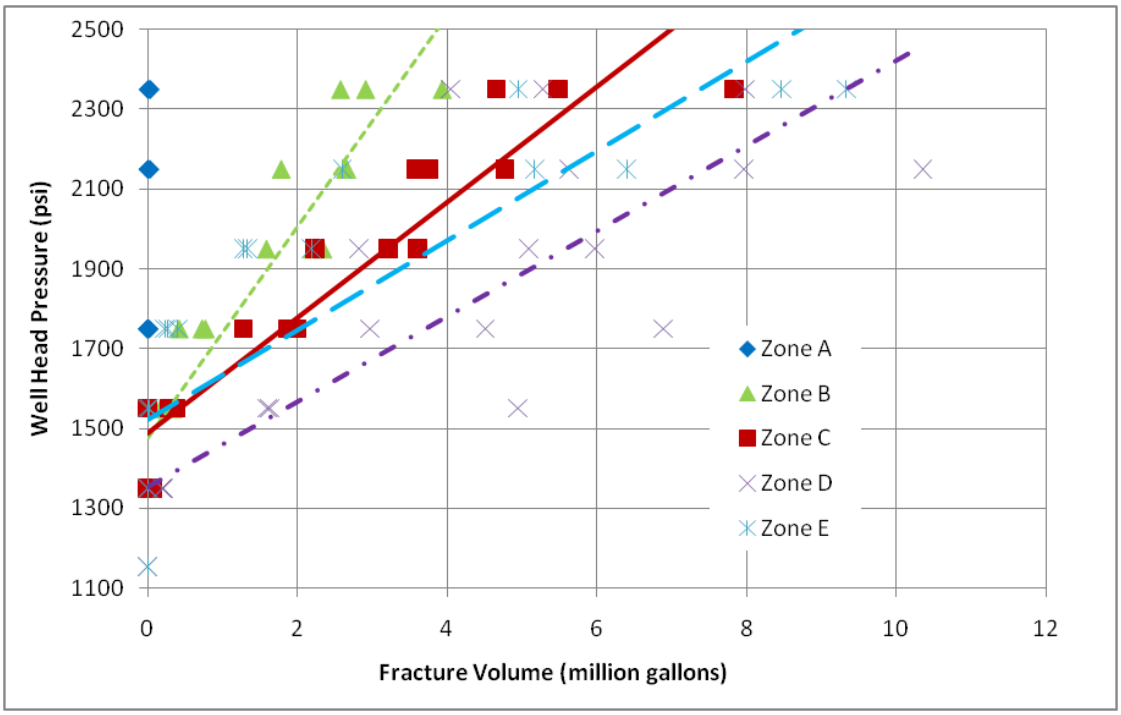

Figure 1: Total fracture volume (injected volume) for five different wellhead pressures in each of the different zones. Top graph is for 0.66 psi/ft S_{hmin} stress case and bottom graph is for 0.70 psi/ft S_{hmin} stress case. Three points at each pressure for each zone represent the different stochastic realizations. The slope of the linear fits is a measure of the efficacy of stimulation in each zone, and the zero volume intercept shows the pressure where, on average, hydroshearing initiates for that zone.

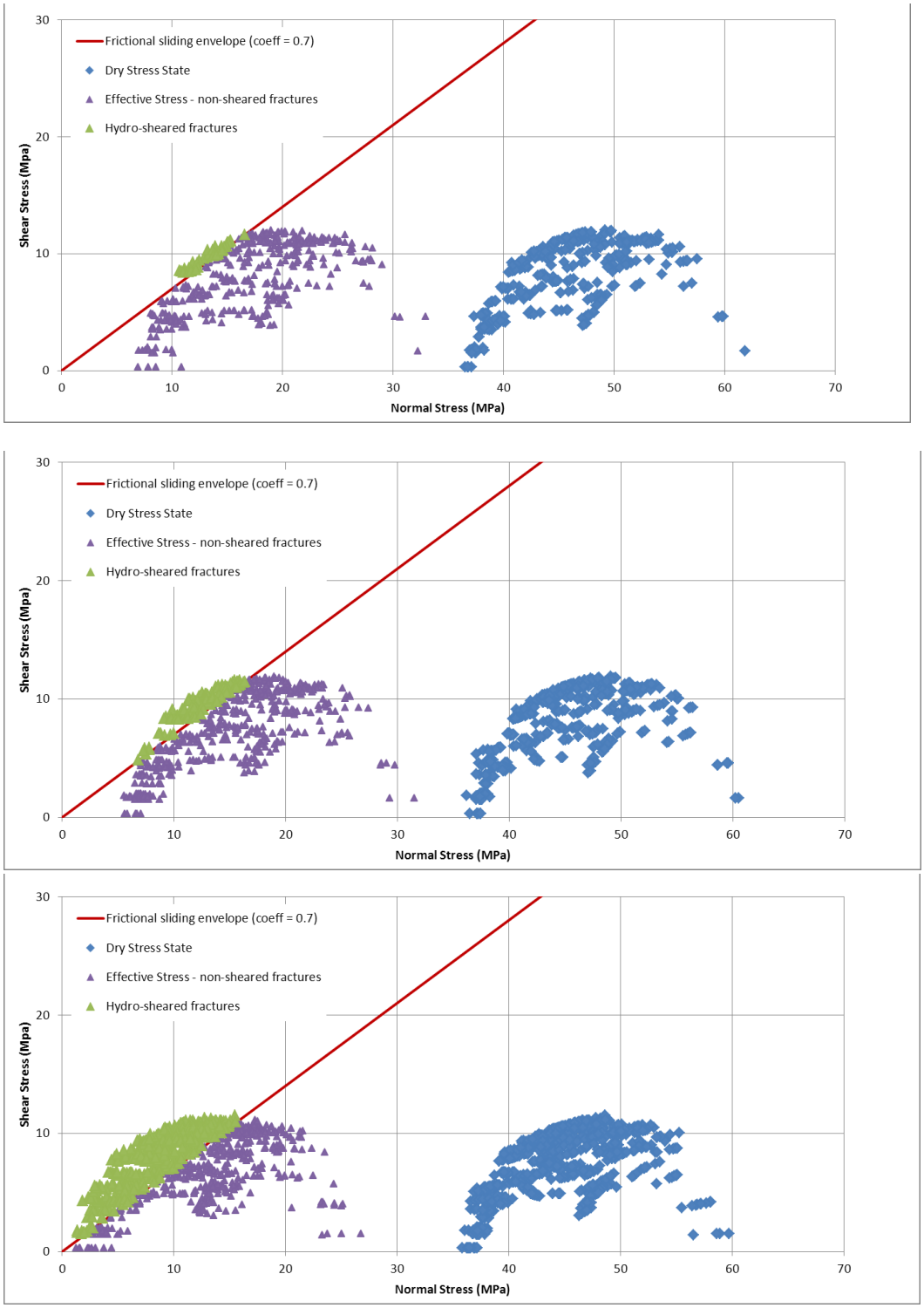

Figure 2: Mohr circle plots for Zone C, stress case 0.66 psi/ft S_{hmin} at: (top) 1153 psi WHP (7.9 MPa), (middle) 1350 psi WHP (9.3 MPa) and (bottom) 1950 psi WHP (13.4 MPa).

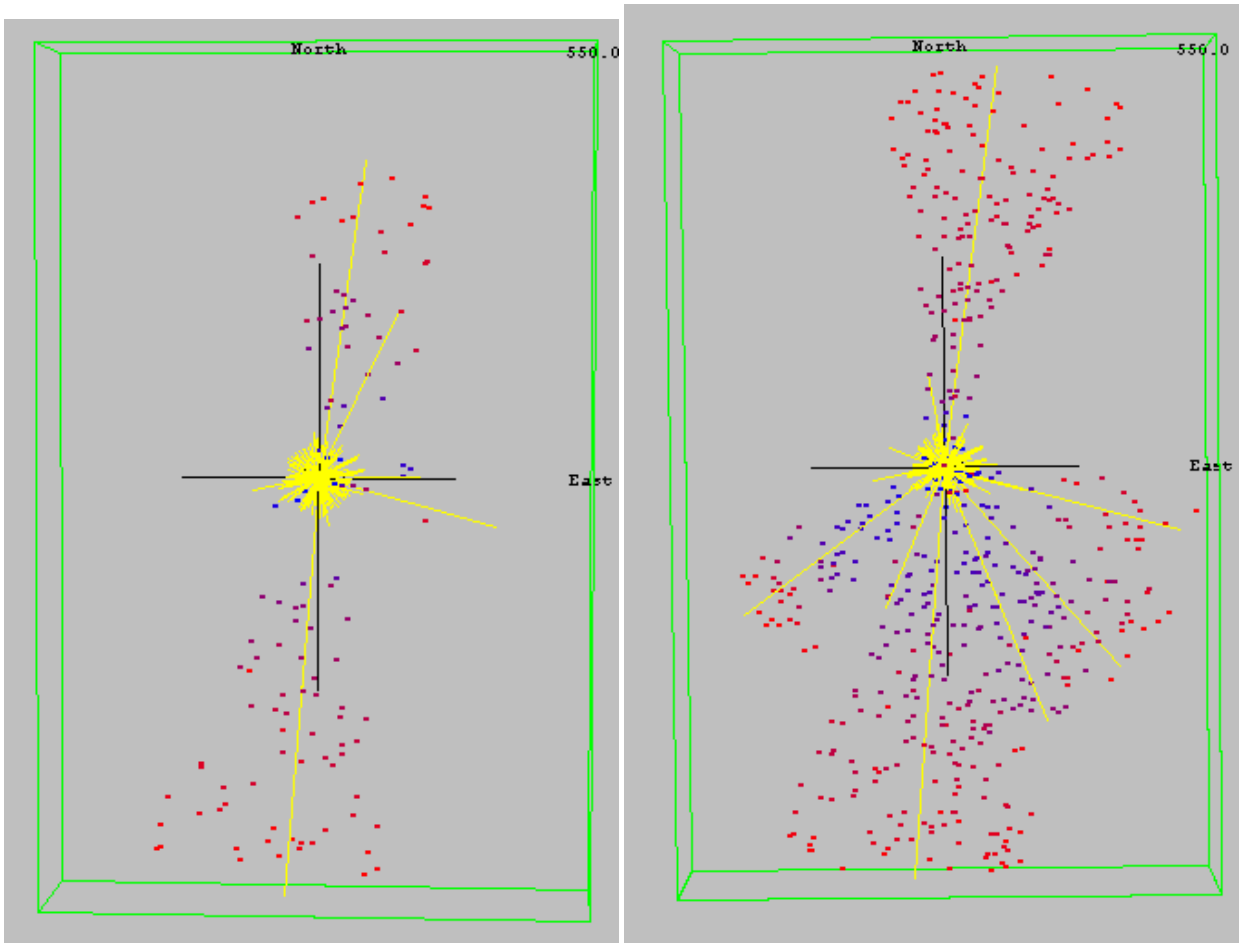

Figure 3: Map view with north on top of modeled microseismicity cloud for one model realization of Zone C: (left) at 1350 psi (9.3 MPa) WHP, and (right) 1950 psi (13.4 MPa) WHP. Fracture volume for model on the left is 710 thousand gallons (2700 m^3). Fracture volume for the model on the right is 6.0 million gallons (23,000 m^3).

fractures cross the frictional failure envelope (green triangles in Figure 2). On average, a 5.5 million-gallon fracture zone is created at 1950 psi that is wider than the zone created at a pressure closer to the critical hydroshearing pressure. In Figure 3 compare the simulated seismic cloud generated at 1350 psi WHP on the left to that generated at 1950 psi WHP on the right.

Zone D

As indicated on Figure 1, Zone D consistently presents the most attractive EGS stimulation zone at all wellhead pressures. This result is partly due to the five dike margins included into the model that are ideally oriented for shear failure with respect to the minimum principle stress direction. The role of the dike margins can be seen in an image of the induced microseismicity (Figure 4) as steeply dipping seismic streaks. The Zone D model also includes background fractures, which account for most of the horizontal growth of the EGS reservoir in this zone.

Zone E

The results for Zone E are similar to results for Zone C, because these two zones share a fracture model (same fracture intensity, orientations, and sliding frictions). This assumption was made because no fracture data exists for Zone E because the BHTV was not able to log below Zone D (too hot). Like Zone C, Zone E is adjacent to the granodiorite dikes and dominated by basalt with minor felsic diking.

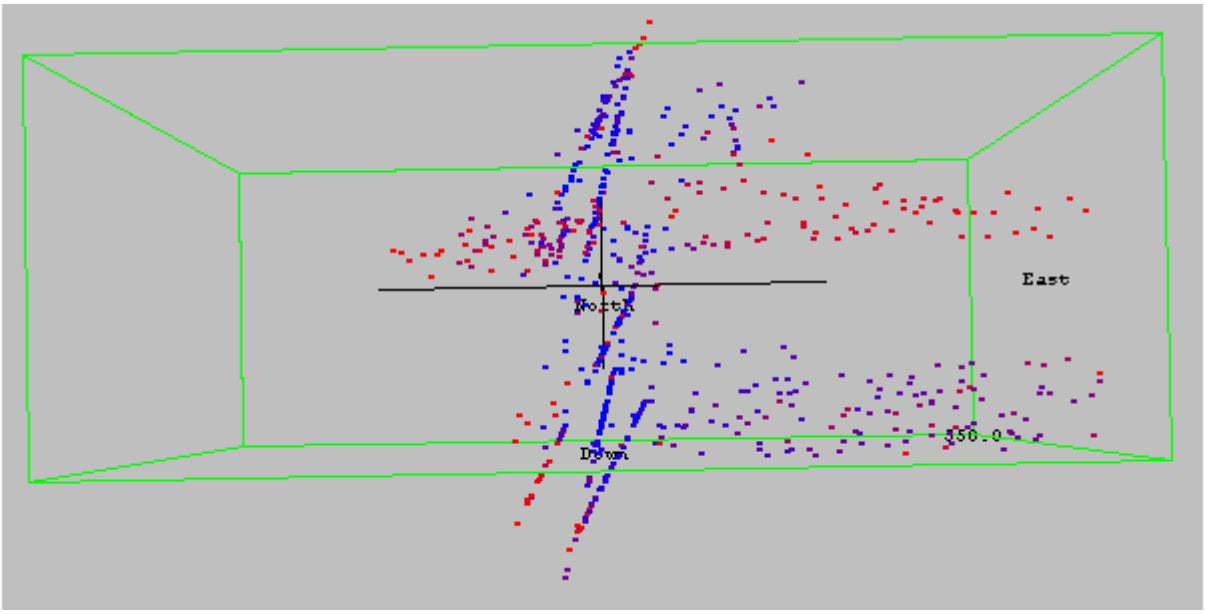

Figure 4: Cross sectional view looking north of modeled microseismicity for Zone D at 1950 psi WHP at the end of model run. Deterministic dike margins can be seen as west-dipping seismic streaks. Microseismicity on background fractures grew with southeast and northwest lobes, which shows as east and west growth in this cross-sectional view.

All Zones

To visualize the complete stimulation, the simulated microseismicity for all the zones was combined into a single 3D visualization (Figure 5). For both stress cases (Table 3), the total volumes are about 22 million gallons (83,000 m^3), so this could be considered an end result after 21-day stimulation of multiple zones at about 1 million gallons per day (694 gpm, 44 L/s). Fracturing multiple zones in a single open-hole interval, as has been modeled using AltaStim, will require the use of AltaRock's proprietary diverters for zonal isolation.

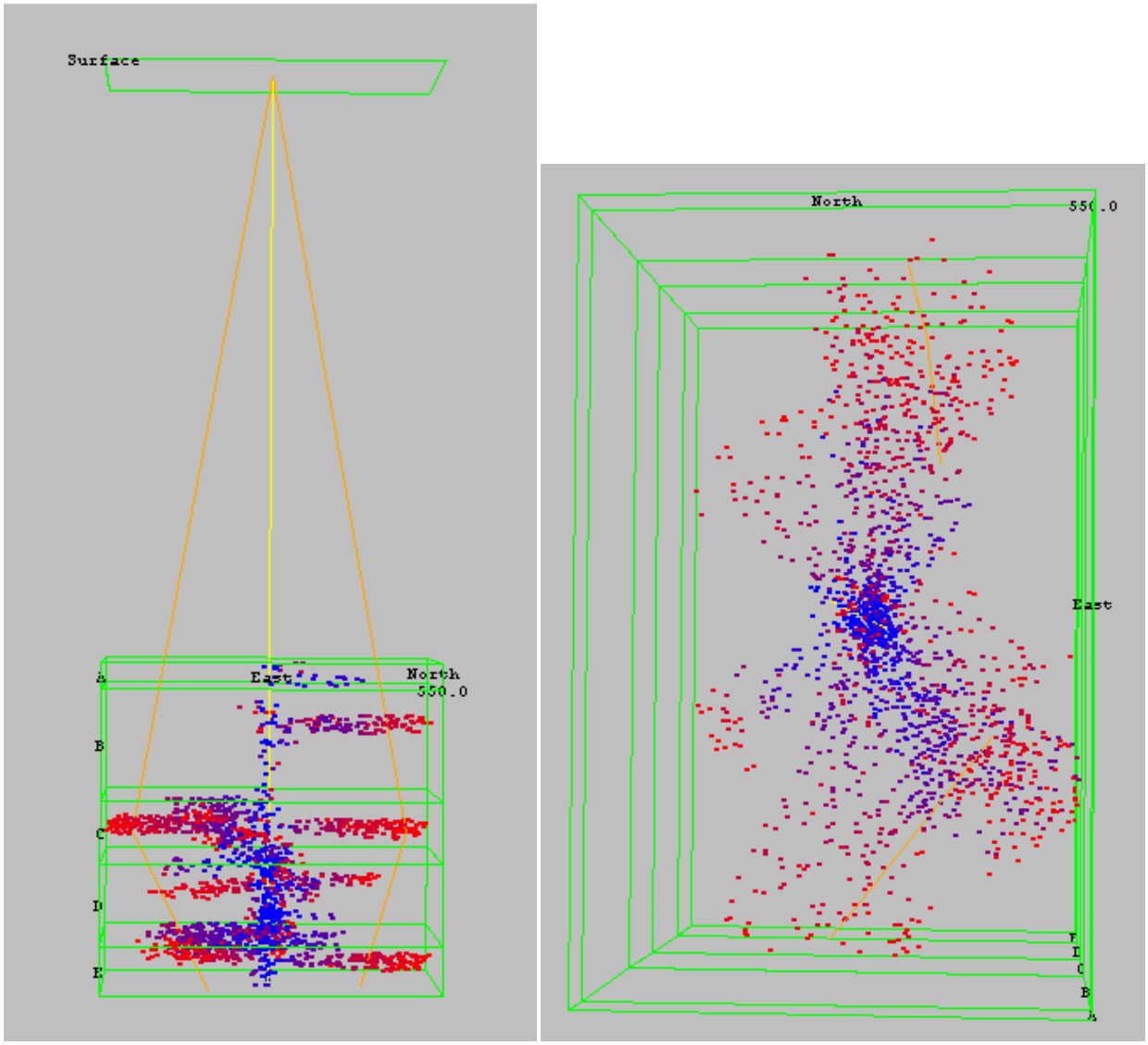

Figure 5: Combined microseismicity for all five zones; (left) scaled view looking west includes surface and wells courses of injector (yellow) and producers (orange), and (right) map view of combined microseismicity.

Table 3: Total volume for combined model of all zones.

	Stress case 1 0.66 psi/ft S_{hmin}	Stress case 2 0.70 psi/ft S_{hmin}
WHP (psi)	Total Volume (Million gallons)	Total Volume (Million gallons)
1153	0.4	0.0
1350	5.5	0.2
1550	10.2	3.2
1750	15.6	7.5
1950	22.1	11.3
2150		19.1
2350		22.5

Conclusions

With a native state close to failure (0.66 psi/ft S_{hmin}), 1350 psi WHP will initiate hydroshearing in all model zones except Zone A, the least fractured portion of the well bore. A WHP of 1950 psi can create several distinct EGS fracture zones to meet the goals of each stimulation stage: over 5 million gallons injected per stage, ~550 m half-length (Figure 1 – top). With a native state further from failure (0.70 psi/ft S_{hmin}), the results are similar except that an additional 200 psi of pressure is needed initiate hydroshearing (1950 psi) and meet the stimulation's objectives (2150 psi) (Figure 1 – bottom).

In the model, it is possible to reach the EGS reservoir length goal (>500 m) without reaching the EGS reservoir volume goal (over 5 million gallons). This result occurs when the wellhead pressure is high enough to initiate hydroshearing, but the orientation range of the stimulated fractures is narrow, resulting in a thin, low volume reservoir (Figure 3 – left). The most attractive modeled reservoirs resulted when the pressures were well into the hydroshearing regime and just below the hydrofracking or tensile failure regime.

Relatively low fracture intensity and high coefficient of sliding friction (μ=0.85) of silicic extrusive volcanic rocks (tuff, rhyolite, and dacite) may suppress hydroshearing in the upper two zones (A and B). The Zone D model, populated with ideally oriented, weaker dike margins, produces the highest volume EGS reservoirs and requires the lowest pressures. EGS reservoirs in Zones C and E, the zones with the highest modeled fracture intensities, also produce high

volume EGS reservoirs. The modeling effort presented here is not complete. Additional AltaStim models will be run in advance of the actual EGS demonstration as further data and analysis becomes available.

Acknowledgment
This material is based on work supported by the Department of Energy under Award Number DE-EE0002777.

References

Davatzes, N. and S. Hickman, this volume, Preliminary Analysis of Fractures, Strength, and Stress Directions in the Newberry EGS Well NWG 55-29.

Jing, Z., J. Willis-Richards , K. Watanabe, and T. Hashida, 2000, A three-dimensional stochastic rock mechanics model of engineered geothermal systems in fractured crystalline rock. *J. Geophy. Res.* 105, B10, pp. 23663-23679.

Lockner, D. A., and N. M. Beeler, 2002, Rock failure and earthquakes, in W. K. Lee, H. Kanamori, P. Jennings, and C. Kisslinger, eds., International handbook of earth- quake and engineering seismology: San Diego, California, Academic Press, v. 81A, p. 505–537.

Morrow, C. and J. Byerlee, 1984, Frictional sliding and fracture behavior of some Nevada Test Site tuffs, Proceedings of the U.S. Symposium on Rock Mechanics, 25th, p. 467-474.

Osborn, W.L., S. Petty, T.T. Cladouhos, J. Iovenitti, L. Nofziger, O. Callahan1, D. Perry and P. L. Stern, this volume, Newberry Volcano EGS Demonstration – Phase I Results.

Willis-Richards, J., K. Watanabe and H. Hashida, 1996, Progress toward a stochastic rock mechanics model of engineered geothermal systems. *J. Geophy. Res.* 101, B8, pp. 17481-17496.